Nonlinear quantum effects in electromagnetic radiation of a vortex electron

D. V. Karlovets [1] and A. M. Pupasov-Maksimov [2]
[1] *Tomsk State University, Lenina Avenue 36, 634050 Tomsk, Russia*
[2] *Universidade Federal de Juiz de Fora, 36036-900, Juiz de Fora, Brasil*

(Received 7 September 2020; accepted 23 December 2020; published 19 January 2021)

There is a controversy of how to interpret interactions of electrons with a large spatial coherence with light and matter. When such an electron emits a photon, it can do so either as if its charge were confined to a point within a coherence length, the region where a square modulus of a wave function $|\psi|^2$ is localized, or as a continuous cloud of space charge spread over it. This problem was addressed in a recent study [R. Remez *et al.*, Phys. Rev. Lett. **123**, 060401 (2019)] where a conclusion was drawn in favor of the first (point) interpretation. Here we argue that there is an alternative explanation for the measurements reported in that paper, which relies on a purely classical concept of a so-called prewave zone and does not allow one to refute the second interpretation. We propose an experiment of Smith-Purcell radiation from a nonrelativistic vortex electron carrying orbital angular momentum, which can unambiguously lead to the opposite conclusion. Beyond the paraxial approximation, the vortex packet has a nonpoint electric quadrupole moment, which grows as the packet spreads and results in a nonlinear L^3 growth of the radiation intensity with the length L of the grating when L is much larger than the packet's Rayleigh length. Such a nonlinear effect has never been observed for single electrons and, if detected, it would be a hallmark of the nonpoint nature of charge in a wave packet. Thus, two views on $|\psi|^2$ are complementary to each other and an electron radiates either as a point charge or as a continuous charge flow depending on the experimental conditions and on its quantum state. Our conclusions hold for a large class of non-Gaussian packets and emission processes for which the radiation formation length can exceed the Rayleigh length, such as Cherenkov radiation, transition radiation, diffraction radiation, and so forth.

DOI: 10.1103/PhysRevA.103.012214

I. INTRODUCTION

The particle-wave duality underpinned by de Broglie [1] lies in the core of quantum mechanics. Modern electron microscopes utilize beams the transverse coherence length of which can exceed 1 mm, and in a single-particle regime—for currents lower than 50 nA—the wave nature of individual electrons is expected to reveal itself in electromagnetic radiation generated during the interaction with matter and light. However, it was found in a recent study [2] that optical Smith-Purcell radiation [3] of electrons with a transverse coherence length $\sigma_{\perp}^{(e)}$ larger than 33 μm occurs as if the charge were confined to a point within this length where a square modulus of a wave function $|\psi|^2$ is localized. Similar conclusions were also drawn in Ref. [4] for photoemission in a laser wave, while dependence on the electron packet's size was shown to appear when the photons are in the coherent state [5] or when the electron's state is different from a simplified plane wave [6–11], especially when an electron Wigner function [12] is not everywhere positive [4]. The results of Ref. [2] seem to refute a wavelike interpretation of $|\psi|^2$ according to which the charge e is spread continuously over the entire coherence length akin to a multiparticle beam. On a more fundamental level, the latter interpretation is due to corrections to the classical radiation intensity that arise because of the quantum character of the electron motion and not due to the quantum recoil. These corrections due to the wave packet's shape and size can usually be safely neglected for relativistic particles, which is implied in such quasiclassical approaches as an operator method [13,14] and an eikonal approximation [8].

Here we show that there is an alternative explanation for the measurements reported in Ref. [2], which is based on a purely classical concept of the so-called *prewave zone* [15–17] and, therefore, it does not allow one to conclude in favor of one of the interpretations. We demonstrate how to modify the experimental scheme in order to come to the opposite (continuous current density) conclusion without an alternative classical explanation. Namely, we propose to use the vortex electrons carrying orbital angular momentum (OAM) $\hbar\ell$ [18] to generate Smith-Purcell radiation. Such electrons—unlike the customary Gaussian beams—have an intrinsic electric quadrupole moment beyond a paraxial approximation [19,20], which is proportional to the packet's coherence length, and the wider the packet is the larger the quadrupole contribution to the radiation. Spreading of a nonrelativistic vortex packet during its propagation next to a grating can result in a nonlinear L^3 dependence of the radiation intensity on the grating length L due to the quadrupole moment.

The nonlinear effects have previously been known only for Smith-Purcell radiation from high-current beams, starting from 1 mA [21,22], or for electrons exposed to a laser field [23], but never for a single freely propagating electron. Here we predict a nonlinear enhancement of the quantum corrections to the classical radiation intensity for a single vortex electron or, more generally, for any non-Gaussian packet with a quadrupole moment, which is also the case for an Airy beam [24], for a Schrödinger's cat state, etc. We argue that for the available beams with $\ell \gg 1$ such a nonparaxial quantum effect due to the packet's finite size can be detected and it would be a hallmark of the nonpoint nature of charge in a wave packet, especially when the recoil is vanishing. Importantly, our conclusions hold for a wide class of emission processes for which the radiation formation length can exceed the packet's Rayleigh length, such as transition radiation or diffraction radiation in a slab, emission in a laser pulse of a finite length, and so on. A system of units $\hbar = c = 1$ is used.

II. PREWAVE ZONE EFFECT IN SMITH-PURCELL RADIATION

Smith-Purcell radiation as a special case of diffraction radiation [3,17,25–28] arises as the field of an electron induces a time-varying current density $\boldsymbol{j}$ on a grating. Quantum mechanically, the radiation arises due to elastic scattering of a virtual photon by the grating. The transverse coherence length of the virtual photon emitted by the electron is

$$\sigma_{\perp}^{(\gamma)} \approx \beta\gamma\lambda \lesssim \lambda \text{ for } \beta \approx 0.4\text{–}0.7, \tag{1}$$

where $\gamma = \varepsilon/m = 1/\sqrt{1-\beta^2} \gtrsim 1$. There are at least two reasons why a nonrelativistic electron with a large transverse coherence length

$$\sigma_{\perp}^{(e)} \gg \lambda \gtrsim \sigma_{\perp}^{(\gamma)} \tag{2}$$

emits Smith-Purcell (diffraction) radiation like a point particle confined inside a region of the width $\sigma_{\perp}^{(e)}$ where $|\psi|^2$ is localized and not like a cloud of space charge e spread over this region.

(1) As the radiation is due to scattering of the virtual photons, *a radiation formation width* is of the order of $\sigma_{\perp}^{(\gamma)}$, not the entire region of $\sigma_{\perp}^{(e)}$, which is profoundly different from radiation by an accelerated electron.

(2) If a detector is placed at a far distance, $r \gg \sigma_{\perp}^{(e)}$, a multipole expansion of the radiation intensity holds:

$$\frac{d^2W}{d\omega d\Omega} \equiv dW = dW_e + dW_{e\mu} + dW_{eQ} + dW_{\mu} + dW_Q + \dots, \tag{3}$$

even if the packet is wide. Here dW_e is due to the electron charge e, $dW_{e\mu}$ describes interference of the waves emitted by the charge and by the electron's point magnetic moment [29] $\boldsymbol{\mu}$, dW_{eQ} is due to a *nonpoint* electric quadrupole moment Q_{ij}, etc. In a linear approximation, suitable for currents lower than 1 mA, these multipole moments are coupled to those of the wave packet itself (see Sec. III C below). A key observation here is that all the higher moments *are vanishing* if the packet is Gaussian in its rest frame, at least approximately [19]. That is why, whatever width a packet has, it always radiates like a point charge,

$$dW = dW_e, \tag{4}$$

within the paraxial approximation.

Thus, the conclusions of Ref. [2] could have been expected for the chosen experimental conditions but they do not allow one to unambiguously refute the continuous current density interpretation because the measurements could support it if the conditions were different. Before we formulate them, we demonstrate how the observed in Ref. [2] wide azimuthal distributions can be explained by using a *purely classical* concept of the prewave zone [15–17]. First, the models of Smith-Purcell radiation from a point charge (see, for instance, Refs. [17,26–28]) predict the far-field azimuthal distributions that *are much narrower* than those in Fig. 3 of Ref. [2] (see the black solid line in our Fig. 1). This width is a function of the particle energy due to the envelope

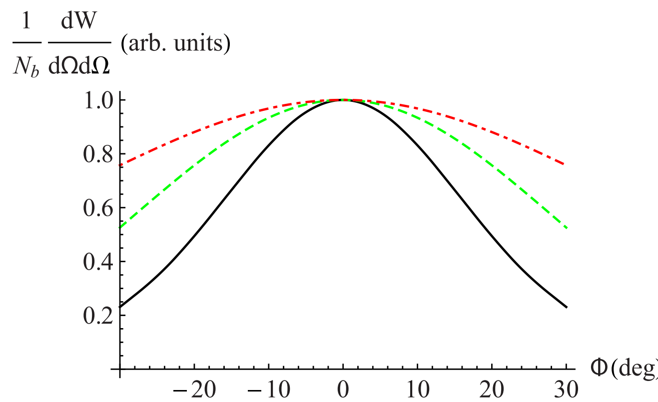

FIG. 1. Azimuthal distributions of Smith-Purcell radiation for $\lambda = d$, the parameters of Ref. [2], and different distances to the detector according to Eq. (8) and the model [31]. The green dashed line ($r = 0.5\, r_{\text{p-w}}$) and the red dash-dotted line ($r = 0.3\, r_{\text{p-w}}$) correspond to the prewave zone, while the black solid line corresponds to the wave zone ($r \gg r_{\text{p-w}}$).

$$dW_e \propto \exp\left\{-\frac{4\pi h}{\beta\gamma\lambda}\sqrt{1+\beta^2\gamma^2\cos^2\Phi\sin^2\Theta}\right\} \tag{5}$$

where h is an impact parameter. This envelope has a kinematical origin and is largely model independent (see Ref. [30]). The distributions wider than those predicted by Eq. (5) can be a hallmark that the measurements were performed in the prewave zone, not in the far field.

When collecting many photons emitted by many electrons, a transverse region of the grating, which participates in the formation of radiation, is of the order of the beam width $\sigma_{\text{b}}^{(e)}$, which is much larger than the width of a packet $\sigma_{\perp}^{(e)}$. So, the condition of the wave zone in a plane $\Theta \approx \Phi \approx \pi/2$ (see Fig. 2) is [16]

$$r \gg r_{\text{p-w}} = \left(\sigma_{\text{b}}^{(e)}\right)^2/\lambda. \tag{6}$$

For parameters of Ref. [2], the prewave zone radius $r_{\text{p-w}}$ is found to be

$$r_{\text{p-w}} \approx 15 \text{ cm},\ \sigma_{\text{b}}^{(e)} = 300\,\mu\text{m}, \\ r_{\text{p-w}} \approx 6.7 \text{ m},\ \sigma_{\text{b}}^{(e)} = 2\,\text{mm}. \tag{7}$$

Thus, the measurements of Ref. [2] are likely to have taken place in the prewave zone where the azimuthal distributions must be very broad [16].

To take this effect into account, one needs to average the one-particle intensity, $dW^{\text{class}}(\mathbf{r}_T)$, not with $|\psi|^2$ as in Eq. (4) of Ref. [2] but with a beam transverse distribution function

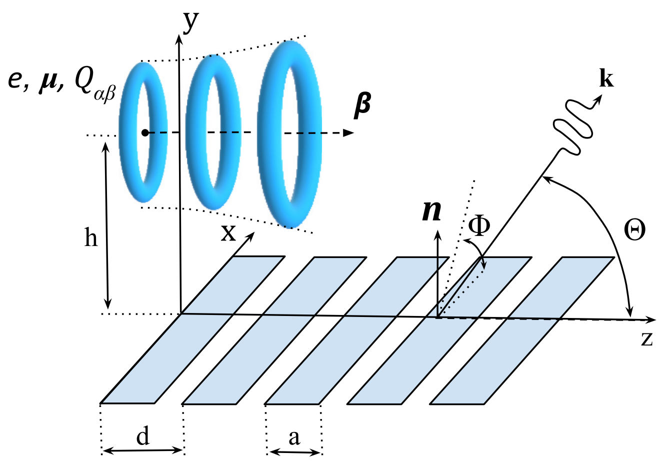

FIG. 2. Smith-Purcell radiation of a vortex electron packet possessing a point charge e, a point magnetic moment $\boldsymbol{\mu}$, and a nonpoint electric quadrupole moment $Q_{\alpha\beta}(t)$, which grows as the packet spreads. The radiation wavelength is $\lambda = d\,(\beta^{-1} - \cos\Theta)/g,\ g = 1, 2, 3, \ldots$.

$\rho_b(\mathbf{r}_T)$:

$$\frac{dW}{d\omega d\Omega} = \int d^2\mathbf{r}_T\, \rho_b(\mathbf{r}_T)\, \frac{dW^{\text{class}}(\mathbf{r}_T)}{d\omega d\Omega}. \tag{8}$$

The function ρ_b can be Gaussian, $\rho_b \propto N_b \exp\{-\mathbf{r}_T^2/2(\sigma_b^{(e)})^2\}$, normalized to a number N_b of electrons in the beam. Importantly, both Eqs. (8) and (4) of Ref. [2] indirectly imply that the detector can be placed in the prewave zone because the far-field intensity does not depend on the transverse shift $\mathbf{r}_T$ at all. Indeed, this shift is a phase rotation,

$$\psi(\mathbf{p}) \to \psi(\mathbf{p})\, e^{-i\mathbf{p}\cdot\mathbf{r}_T}, \tag{9}$$

and the radiation intensity stays invariant under it (see Sec. III B below). Unlike Eq. (8), the wave zone formula deals with the momentum representation, which is quite natural.

To calculate $dW^{\text{class}}(\mathbf{r}_T)$ at an arbitrary distance r we use the model of Ref. [31], although the azimuthal distributions are largely model independent. As can be seen in Fig. 1, the green and red lines fit the data in Fig. 3 of Ref. [2] much better than the far-field line does, which represents an alternative classical explanation of the unusually wide distributions reported in Ref. [2].

III. RADIATION FROM A WAVE PACKET

A. Generalities

Consider radiation of a charged wave packet of arbitrary shape either in external electromagnetic field or when interacting with a medium in the lowest order of the perturbation theory in quantum electrodynamics (QED). The formula (3) is based on a multipole expansion of the transition current density $\mathbf{j}_{fi}$, in which two quantum effects are present: (1) the recoil and (2) the effects of the wave packet's size and shape. The possibility of such a multipole expansion not only in classical electrodynamics but also in QED follows from linearity of the latter on the tree level. Indeed, the radiation intensity of the classical current $j_\mu(x)$ *in the far field* is given by Eq. (14.70) in Ref. [32], which can be written as follows:

$$\frac{d^2W}{d\omega d\Omega} = -\frac{\omega^2}{(2\pi)^2}\, j_\mu(k)[j^\mu(k)]^*, \qquad j_\mu(k) = \int d^4x\, j_\mu(x)\, e^{it\omega - i\mathbf{k}\mathbf{x}}, \tag{10}$$

when integrating over all space and time. A probability to emit a photon by an electron in the lowest order of QED is

$$d\nu = |S_{fi}|^2\, \frac{d^3k}{(2\pi)^3},\ S_{fi} = -ie\int d^4x\, j^\mu_{fi}(x) A^*_\mu(x), \qquad j^\mu_{fi}(x) = \bar{\psi}_f(x)\gamma^\mu\psi_i(x). \tag{11}$$

When the photon is detected in the wave zone as a plane wave with $A_\mu(x) = \frac{\sqrt{4\pi}}{\sqrt{2\omega}}\, e_\mu(k)\, \exp\{-it\omega + i\mathbf{k}\mathbf{x}\}$, the radiated energy summed over the photon polarizations by $e_\mu e^*_\nu \to -g_{\mu\nu}$ is found as

$$\frac{d^2W}{d\omega d\Omega} = \omega\,\frac{d^2\nu}{d\omega d\Omega} = -\frac{\omega^2}{(2\pi)^2}\, e^2 j_{fi_\mu}(k)[j_{fi}{}^\mu(k)]^*. \tag{12}$$

The only difference from Eq. (10) is that the electron final state does not coincide with its initial state, while both these states are arbitrary and are *not necessarily plane waves*. This correspondence is a manifestation of the Bohr's complementarity principle and it is because of this that the general quantum formulas for radiation intensity look similar to those of the classical electrodynamics [see Sec. 45 in Ref. [14]]. This is in particular the case for such a wide class of processes as polarization radiation beyond the dipole approximation, including diffraction and Smith-Purcell radiation, in which the quantum recoil is vanishing but the multipole structure of the current is retained, which means that the "geometric" corrections due to the size and shape of the packet are taken into account (see below).

The contributions of higher multipole moments are described in classical electrodynamics by keeping higher-order terms in expansion of the Green's function into series. Analogously, the multipole expansion of the radiation intensity in QED can be obtained by expanding the plane-wave component $\exp\{-i\mathbf{k}\mathbf{x}\}$ of the final photon into series over the spherical waves—see Sec. 46 and 47 in Ref. [14]. Such a multipole expansion holds irrespective of the specific emission process, also when the recoil is vanishing, which is implied in Eq. (3). As a result, the matrix element S_{fi} in (11) will represent a series over the multipole contributions and the intensity will look like Eq. (3). However, as we show hereafter, for this expansion to have a sense it is important that the current $j^\mu_{fi}(x)$ be spatially localized, which means that both the initial and final electrons are described as wave packets rather than plane waves.

B. Role of the size and shape of the electron packet

Now we are going to demonstrate how to take into account the size and shape of an electron wave packet in radiation or the shape of a beam in *incoherent* radiation of N_b electrons, which is typical in an electron microscope. Let the initial electron be described as an arbitrary packet with a wave function being a superposition of plane waves:

$$\psi_i(x) = \int \frac{d^3p}{(2\pi)^3}\, \psi(\mathbf{p})\, \frac{u_i(p)}{\sqrt{2\varepsilon}}\, e^{-it\varepsilon + i\mathbf{p}\mathbf{x}},$$
$$\bar{u}_i(p)u_i(p) = 2m,\ \varepsilon = \sqrt{\mathbf{p}^2 + m^2}, \tag{13}$$
$$\int d^3x|\psi_i(x)|^2 = \int \frac{d^3p}{(2\pi)^3}|\psi(\mathbf{p})|^2 = 1.$$

The matrix element and the probability to emit a plane-wave photon become

$$S_{fi} = \int \frac{d^3p}{(2\pi)^3}\, \psi(\mathbf{p})\, S_{fi}^{(\mathrm{pw})}(\mathbf{p}),$$
$$d\nu = \int \frac{d^3p}{(2\pi)^3}\frac{d^3p'}{(2\pi)^3}\, \psi(\mathbf{p})\psi^*(\mathbf{p}')\, S_{fi}^{(\mathrm{pw})}(\mathbf{p})\left(S_{fi}^{(\mathrm{pw})}\right)^*(\mathbf{p}')\, \frac{d^3k}{(2\pi)^3}$$
$$= \int \frac{d^3p}{(2\pi)^3}\frac{d^3q'}{(2\pi)^3}\, \psi(\mathbf{p}+\mathbf{q}/2)\psi^*(\mathbf{p}-\mathbf{q}/2)$$
$$\times S_{fi}^{(\mathrm{pw})}(\mathbf{p}+\mathbf{q}/2)\left(S_{fi}^{(\mathrm{pw})}\right)^*(\mathbf{p}-\mathbf{q}/2)\, \frac{d^3k}{(2\pi)^3}, \tag{14}$$

where we use the new variables

$$(\mathbf{p}, \mathbf{p}') \to (\mathbf{p}+\mathbf{q}/2, \mathbf{p}-\mathbf{q}/2). \tag{15}$$

If we deal with a single electron and not with a multiparticle beam, one can completely neglect the dependence of $S_{fi}^{(\mathrm{pw})}$ on $\mathbf{q}$, which is called *the paraxial approximation*. The corrections due to small $\mathbf{q}$ arise beyond the paraxial regime because of the *autocorrelation* of the scattering amplitude or due to its phase ζ_{fi}:

$$S_{fi}^{(\mathrm{pw})}(\mathbf{p}) = \left|S_{fi}^{(\mathrm{pw})}(\mathbf{p})\right| e^{i\zeta_{fi}(\mathbf{p})}.$$

If the phase is constant, which also depends on the final electron state, the corrections vanish exactly. For a beam, the leading term with $|S_{fi}^{(\mathrm{pw})}(\mathbf{p})|^2$ describes the incoherent emission of uncorrelated particles, while the first correction due to nonvanishing $\mathbf{q}$ takes inter particle correlations (coherence effects) into account. The small-$\mathbf{q}$ expansion of $S_{fi}^{(\mathrm{pw})}$ is justified because the electron wave packet is normalized and, therefore, the function $\psi(\mathbf{p})$ can behave at large $\mathbf{p} \to \infty$, for instance, as $\psi(\mathbf{p}) \propto \exp\{-(\mathbf{p} - \langle\mathbf{p}\rangle)^2/2(\delta p)^2\}$. Then

$$\psi^*(\mathbf{p}-\mathbf{q}/2)\psi(\mathbf{p}+\mathbf{q}/2)$$
$$\propto \exp\{-(\mathbf{p} - \langle\mathbf{p}\rangle)^2/(\delta p)^2 - \mathbf{q}^2/(2\delta p)^2\} \tag{16}$$

at large $\mathbf{p}$.

The leading term in the paraxial approximation is thus

$$d\nu^{(\mathrm{incoh})} = \int \frac{d^3p}{(2\pi)^3}\frac{d^3q'}{(2\pi)^3}\, \psi(\mathbf{p}+\mathbf{q}/2)\psi^*(\mathbf{p}-\mathbf{q}/2)$$
$$\times \left|S_{fi}^{(\mathrm{pw})}(\mathbf{p})\right|^2 \frac{d^3k}{(2\pi)^3}$$
$$= \int \frac{d^3p}{(2\pi)^3}\, n(\mathbf{0}, \mathbf{p}, 0)\, d\nu^{(\mathrm{pw})}(\mathbf{p}), \tag{17}$$

or for the radiation intensity in the wave zone [see Eqs. (3) and (4) in Ref. [4]]

$$\frac{dW^{(\mathrm{incoh})}}{d\omega d\Omega} = \int \frac{d^3p}{(2\pi)^3}\, n(\mathbf{0}, \mathbf{p}, 0)\, \frac{dW^{(\mathrm{pw})}(\mathbf{p})}{d\omega d\Omega}, \tag{18}$$

where we have used the definition of a Wigner function [12]:

$$n(\mathbf{x}, \mathbf{p}, t) = \int \frac{d^3q}{(2\pi)^3}\, \psi^*(\mathbf{p}-\mathbf{q}/2, t)\psi(\mathbf{p}+\mathbf{q}/2, t)\, e^{i\mathbf{q}\mathbf{x}},$$
$$\psi(\mathbf{p}, t) = \psi(\mathbf{p})\, e^{-it\varepsilon(\mathbf{p})}. \tag{19}$$

The formula (18) allows one to exactly take into account the spatial shape and width of the radiating packet because the momentum uncertainty δp is connected with the former as $\sigma_\perp^{(e)} = 1/\delta p$. Importantly, it is only for a Gaussian packet that the Wigner function $n(\mathbf{0}, \mathbf{p}, 0)$ coincides with $|\psi(\mathbf{p})|^2$ [see Eq. (3) in Ref. [4]], while for a vortex electron, for instance, it does not—see Eq. (68) in Ref. [33]. Thus, for non-Gaussian electron packets equations (17) and (18) also depend on a phase $\varphi(\mathbf{p})$ of the electron wave function

$$\psi(\mathbf{p}) = |\psi(\mathbf{p})|\, e^{i\varphi(\mathbf{p})} \tag{20}$$

and they are applicable for packets with the not-everywhere positive Wigner functions—say, Schrödinger's cat states, coherent superpositions of vortex states, etc.

The main difference of Eq. (18) from Eq. (4) in Ref. [2] is that the former uses the momentum representation, while the latter uses the coordinate one. The use of the momentum representation is natural and even *unavoidable* for the wave zone because the radiation source is completely delocalized, which is why one has to deal with momenta, not coordinates. As clearly seen from Eq. (11), the far-field radiation probability does not depend on the transverse shift $\mathbf{r}_T$ of the radiating electron because such a shift changes only the phase of both the initial and final electrons as

$$\psi_{i,f}(\mathbf{p}) \to \psi_{i,f}(\mathbf{p})\, e^{-i\mathbf{p}\cdot\mathbf{r}_T},$$

to which the intensity is not sensitive. The intensity *is* sensitive, however, to a phase rotation of the initial electron alone, $\psi(\mathbf{p}) \to \psi(\mathbf{p})\, e^{i\varphi(\mathbf{p})}$, which is why the higher multipole moments can make a nonvanishing contribution to the far field. We would like to emphasize that the quantum state of the final electron is *not specified* here and the final photon is described as a delocalized plane wave, which means that the photon is detected in the wave zone. If the final electron were also described as a plane wave, which means that it is not detected, the radiation intensity would *not* depend on the phase $\varphi(\mathbf{p})$ of the initial electron when integrating over all space and time from $-\infty$ to $+\infty$. Such a phase dependence takes place only if the final electron is also described as a spatially localized wave packet, which means that it is detected at a certain distance (not too far) from the radiation region. It is this case which is the most natural for comparison with the classical theory because the transition current $j_{fi}^{\mu}(x)$ is spatially localized, while for the plane-wave final electron it is not so and, therefore, the wave zone *cannot* be defined [34].

For emission of many photons by a beam of electrons, the Wigner function is normalized to a number N_b of particles in the beam:

$$\int \frac{d^3p}{(2\pi)^3}\, n(\mathbf{0}, \mathbf{p}, 0) = N_b.$$

In this case, Eq. (18) describes incoherent radiation, which is a good approximation for small radiation wavelengths $\lambda \ll \sigma_b^{(e)}$ and the low-current (single-electron) regime, typical for electron microscopes. The opposite case of $\lambda \gtrsim \sigma_b^{(e)}$ and the bunched electrons can be realized in a particle accelerator, for which the leading term (18) is no longer sufficient (see Ref. [35]).

In contrast, to describe the radiation in the prewave zone it is natural to use the coordinate representation. The corresponding classical formula is

$$\frac{dW}{d\omega d\Omega} = \int d^2\mathbf{r}_T\, \rho_b(\mathbf{r}_T)\, \frac{dW^{\text{class}}(\mathbf{r}_T)}{d\omega d\Omega}. \tag{21}$$

When the detector is in the far field, the dependence of dW^{class} on $\mathbf{r}_T$ vanishes and we are left with

$$\frac{dW^{\text{far-field}}}{d\omega d\Omega} = N_b\, \frac{dW^{\text{class}}}{d\omega d\Omega}, \tag{22}$$

which reflects the well-known fact that an incoherent form factor for a beam equals unity [35,36]. As has been recently shown in Ref. [36], the incoherent form factor *can differ from unity* when the grating in Smith-Purcell radiation or a target in transition and diffraction radiation is spatially limited—say, when the grating has a width smaller than the transverse coherence length of the virtual photon $\beta\gamma\lambda$, so the radiation formation width is defined by the geometrical sizes of the target.

Analogously, the prewave effect also comes about due to the finite radiation formation width but because the detector is moved closer to the target. Equation (21) explicitly demonstrates, therefore, that the incoherent form factor *also differs from unity* for the radiation in the prewave zone. In this sense, the wide azimuthal distributions measured in Ref. [2] can be treated as an evidence of such a form factor. This conclusion holds not only for Smith-Purcell radiation, but also for a much wider class of emission processes, including diffraction radiation, Cherenkov radiation, transition radiation, Compton and Thomson scattering in laser fields, and so forth.

C. The quasiclassical regime of emission by a wave packet

Now we are going to demonstrate how to study emission in a regime in which the quantum effects are small and treated as corrections to the classical formula. Along with the recoil, these corrections depend on the shape and size of the electron wave packet via the multipole expansion. Both these effects are inherently quantum, so the separation of them in radiation intensity is a rather delicate task even for the Gaussian packets—see, for instance, [9–11]. However when the quantum numbers defining the shape of a non-Gaussian packet are large—say, $\ell \gg 1$ for a vortex electron—the emission is always *quasiclassical* [14] and one can neglect the spin contribution $[\mathcal{O}(\omega/\varepsilon)]$ compared to the contributions originating from the non-Gaussianity of the packet. For the vortex packet with $\ell \gg 1$, such a quasiclassical regime of emission implies (see also Ref. [37])

$$\frac{\omega}{\varepsilon} \ll 1,\ |\ell|\,\frac{\omega}{\varepsilon} \lesssim 1. \tag{23}$$

Thus the geometric corrections to the classical intensity due to the wave packet's shape and size are $|\ell|$ times enhanced compared to those due to recoil.

We start again with the general matrix element

$$S_{fi} = -ie \int d^4x\, j^{\mu}_{fi}(x) A^*_{\mu}(x), \quad j^{\mu}_{fi}(x) = \bar{\psi}_f(x)\gamma^{\mu}\psi_i(x), \tag{24}$$

and take both the incoming electron and the final electron as some wave packets:

$$\psi_i(x) = \int \frac{d^3p}{(2\pi)^3}\, \psi_i(\mathbf{p})\, \frac{u_i(p)}{\sqrt{2\varepsilon_i}}\, e^{-it\varepsilon_i + i\mathbf{p}\mathbf{x}},\ \bar{u}_i(p)u_i(p) = 2m,$$
$$\psi_f(x) = \int \frac{d^3p}{(2\pi)^3}\, \psi_f(\mathbf{p})\, \frac{u_f(p)}{\sqrt{2\varepsilon_f}}\, e^{-it\varepsilon_f + i\mathbf{p}\mathbf{x}},\ \bar{u}_f(p)u_f(p) = 2m. \tag{25}$$

Depending on the external field, these packets can be coherent superpositions of the Volkov states in a plane wave, of the Landau states in magnetic field, etc. The transition current looks as follows:

$$\begin{aligned} j^{\mu}_{fi}(x) &= \int \frac{d^3p}{(2\pi)^3}\frac{d^3p_f}{(2\pi)^3}\, \psi^*_f(\mathbf{p}_f)\psi_i(\mathbf{p})\, \frac{\bar{u}_f(\mathbf{p}_f)}{\sqrt{2\varepsilon_f}} \\ &\quad\times \gamma^{\mu}\frac{u_i(\mathbf{p})}{\sqrt{2\varepsilon_i}}\, e^{-ix(p-p_f)} \\ &= \int \frac{d^3p}{(2\pi)^3}\frac{d^3q}{(2\pi)^3}\, \frac{\psi^*_f(\mathbf{p}-\mathbf{q}/2)}{\sqrt{2\varepsilon(\mathbf{p}-\mathbf{q}/2)}}\, \frac{\psi_i(\mathbf{p}+\mathbf{q}/2)}{\sqrt{2\varepsilon(\mathbf{p}+\mathbf{q}/2)}} \\ &\quad\times \bar{u}_f(\mathbf{p}-\mathbf{q}/2)\,\gamma^{\mu}u_i(\mathbf{p}+\mathbf{q}/2) \\ &\quad\times \exp\{-it[\varepsilon(\mathbf{p}+\mathbf{q}/2) - \varepsilon(\mathbf{p}-\mathbf{q}/2)] + i\mathbf{x}\mathbf{q}\}, \end{aligned} \tag{26}$$

where we again use the variables (15) and no approximations are used at this stage. The indices i and f denote all the remaining quantum numbers the packets can possess (spin, orbital angular momentum, etc.)

Now we notice that the variable $\mathbf{q} = \mathbf{p} - \mathbf{p}_f$ is a momentum transfer for each plane-wave component comprising the wave packets. The large values $|\mathbf{q}| \gg \delta p$ are suppressed in the quasiclassical case $f \to i$ analogously to Eq. (16). However, even in the general quantum regime the large momentum transfers are attenuated by the rapidly oscillating exponent $\exp\{i\mathbf{x}\mathbf{q}\}$. So the effective values of $\mathbf{q}$ are

$$|\mathbf{q}| \lesssim 1/|\mathbf{x}| \sim 1/\sigma_{\perp} = \delta p, \tag{27}$$

whatever shape the packets have.

An expansion of the bispinors into series over $\mathbf{q}$ yields (i and f are just spin indices here)

$$\bar{u}_f(\mathbf{p}-\mathbf{q}/2)\,\gamma^{\mu}u_i(\mathbf{p}+\mathbf{q}/2) = \bar{u}_f(\mathbf{p})\gamma^{\mu}u_i(\mathbf{p}) + \frac{\mathbf{q}}{2}\left(\bar{u}_f(\mathbf{p})\gamma^{\mu}\frac{\partial u_i(\mathbf{p})}{\partial \mathbf{p}} - \frac{\partial \bar{u}_f(\mathbf{p})}{\partial \mathbf{p}}\gamma^{\mu}u_i(\mathbf{p})\right) + \mathcal{O}(\mathbf{q}^2). \tag{28}$$

The first correction *due to recoil* here depends on the electron spin [38] $\boldsymbol{\zeta}$, and in the quasiclassical regime with $f \to i$ (no spin flip) it looks as follows (we omit the index i) [39]:

$$\bar{u}(\mathbf{p})\gamma^{\mu}\frac{\partial u(\mathbf{p})}{\partial p_j} - \frac{\partial \bar{u}(\mathbf{p})}{\partial p_j}\gamma^{\mu}u(\mathbf{p}) = 2i\left\{\frac{1}{\varepsilon+m}\,[\boldsymbol{\zeta}\times\mathbf{p}]_j,\ \frac{p_j}{\varepsilon}\,\frac{\boldsymbol{\zeta}\times\mathbf{p}}{\varepsilon+m} + \mathbf{e}_j\times\boldsymbol{\zeta},\right\}, \tag{29}$$

where $\mathbf{e}_j$ is a unit vector along the jth axis. So, this correction is generally attenuated as $\omega/\varepsilon \ll 1$, coincides with the corresponding term in Eq. (2.4) of Ref. [9], and vanishes for an unpolarized electron. Therefore, for an unpolarized electron we have simply

$$\bar{u}_f(\mathbf{p}-\mathbf{q}/2)\,\gamma^{\mu}u_i(\mathbf{p}+\mathbf{q}/2) \to 2p^{\mu} = 2mu^{\mu}, \tag{30}$$

even if the recoil is not vanishing. In this case, the integral over $\mathbf{q}$ in (26) yields the following function:

$$\tilde{n}(\mathbf{x},\mathbf{p},t) = \int \frac{d^3q}{(2\pi)^3}\,\frac{\psi^*(\mathbf{p}-\mathbf{q}/2,t)}{\sqrt{2\varepsilon(\mathbf{p}-\mathbf{q}/2)}}\,\frac{\psi(\mathbf{p}+\mathbf{q}/2,t)}{\sqrt{2\varepsilon(\mathbf{p}+\mathbf{q}/2)}}\,e^{i\mathbf{q}\mathbf{x}}, \tag{31}$$

which is very similar to the electron Wigner function Eq. (19), but transforms differently under the Lorentz boosts. So the current for an polarized electron looks like

$$j^{\mu}_{f\to i}(x) = \int \frac{d^3p}{(2\pi)^3}\,2p^{\mu}\,\tilde{n}(\mathbf{x},\mathbf{p},t) \tag{32}$$

and depends on the electron's phase φ. We stress that this current is *not fully classical* because the quantum recoil and the packet's phase are taken into account, but the remaining quantum numbers (say, orbital angular momentum) do not change during the radiation.

Let us now analyze effects of the packet's shape and size for an unpolarized electron. The former are defined by the phase φ, while the latter arise due to the finite momentum width $\delta p = 1/\sigma_{\perp}^{(e)} \equiv 1/\sigma_{\perp}$. Let us first denote

$$\Psi(\mathbf{p}) = \frac{\psi(\mathbf{p})}{\sqrt{2\varepsilon(\mathbf{p})}}. \tag{33}$$

Then we represent the new wave functions according to Eq. (20) and find

$$\Psi^*(\mathbf{p}-\mathbf{q}/2)\Psi(\mathbf{p}+\mathbf{q}/2) = \left\{|\Psi|^2 + \frac{1}{4}\,q_iq_j\left[|\Psi|\frac{\partial^2|\Psi|}{\partial p_i\partial p_j} - \left(\frac{\partial|\Psi|}{\partial p_i}\right)\left(\frac{\partial|\Psi|}{\partial p_j}\right)\right] + \mathcal{O}(q^4)\right\}\exp\left\{i\mathbf{q}\frac{\partial\varphi}{\partial\mathbf{p}} + \mathcal{O}(q^3)\right\}, \tag{34}$$

where $\Psi \equiv \Psi(\mathbf{p})$, $\varphi \equiv \varphi(\mathbf{p})$. The exponent here is due to electric and magnetic *dipole moments* of the packet. The mean value of the former is [19]

$$\mathbf{d} = -\left\langle\frac{\partial\varphi(\mathbf{p})}{\partial\mathbf{p}}\right\rangle. \tag{35}$$

However, the true *intrinsic* electric dipole moment of an electron packet is vanishing as it is prohibited by the CPT theorem of the standard model. The mean value of the electric moment (but not of the magnetic one) can be killed by shifting the origin of coordinates or by the choice of initial conditions $\mathbf{x}_0$ [19], which implies the following phase rotation:

$$\Psi \to \Psi\ \exp\{-i\mathbf{x}_0\mathbf{p}\},\ \ \mathbf{x}_0 = -\mathbf{d} = \left\langle\frac{\partial\varphi}{\partial\mathbf{p}}\right\rangle. \tag{36}$$

As a result, we have instead

$$\Psi^*(\mathbf{p}-\mathbf{q}/2)\Psi(\mathbf{p}+\mathbf{q}/2) = \left\{|\Psi|^2 + \frac{1}{4}\,q_iq_j\left[|\Psi|\frac{\partial^2|\Psi|}{\partial p_i\partial p_j} - \left(\frac{\partial|\Psi|}{\partial p_i}\right)\left(\frac{\partial|\Psi|}{\partial p_j}\right)\right] + \mathcal{O}(q^4)\right\}\exp\left\{i\mathbf{q}\left(\frac{\partial\varphi}{\partial\mathbf{p}} - \left\langle\frac{\partial\varphi}{\partial\mathbf{p}}\right\rangle\right) + \mathcal{O}(q^3)\right\}. \tag{37}$$

This ambiguity—that is, dependence of the matrix element on the initial conditions—is well-known (see, for instance, [7,8]) and for a non-Gaussian packet such a choice of the origin guarantees that we work with intrinsic values of the multipole moments.

One can also expand the energies in the exponent as follows:

$$\varepsilon(\mathbf{p}+\mathbf{q}/2) - \varepsilon(\mathbf{p}-\mathbf{q}/2) = \mathbf{q}\mathbf{u} + \mathcal{O}(\mathbf{q}^3),\ \ \mathbf{u} \equiv \mathbf{u}(\mathbf{p}) = \frac{\mathbf{p}}{\varepsilon(\mathbf{p})}. \tag{38}$$

After this, the integral over $\mathbf{q}$ yields a delta function and the current looks as follows (note that we use both ψ and $\Psi = \psi/\sqrt{2\varepsilon}$ here):

$$\begin{aligned}
j^{\mu}_{f\to i}(x) &= \int \frac{d^3p}{(2\pi\hbar)^3}\,\frac{p^{\mu}}{\varepsilon}\left(|\psi|^2 + \frac{1}{4}D_{ij}\,\hat{p}_i\hat{p}_j + \mathcal{O}(\hbar^4)\right)\delta\left[\mathbf{x} - \mathbf{u}t + \hbar\left(\frac{\partial\varphi}{\partial\mathbf{p}} - \left\langle\frac{\partial\varphi}{\partial\mathbf{p}}\right\rangle\right)\right]\\
&\equiv \int \frac{d^3p}{(2\pi\hbar)^3}\left(|\psi|^2 + \frac{1}{4}D_{ij}\,\hat{p}_i\hat{p}_j + \mathcal{O}(\hbar^4)\right)j^{\mu}_{\text{quasi-cl.}}(\mathbf{x},\mathbf{p},t;\hbar),\\
j^{\mu}_{\text{quasi-cl.}}(\mathbf{x},\mathbf{p},t;\hbar) &= \frac{p^{\mu}}{\varepsilon}\,\delta\left[\mathbf{x} - \mathbf{u}t + \hbar\left(\frac{\partial\varphi}{\partial\mathbf{p}} - \left\langle\frac{\partial\varphi}{\partial\mathbf{p}}\right\rangle\right)\right],\\
D_{ij} &= 2\varepsilon\left[|\Psi|\frac{\partial^2|\Psi|}{\partial p_i\partial p_j} - \left(\frac{\partial|\Psi|}{\partial p_i}\right)\left(\frac{\partial|\Psi|}{\partial p_j}\right)\right],
\end{aligned} \tag{39}$$

where $\hat{\mathbf{p}} = -i\hbar\nabla$ and we have restored Planck's constant $\hbar$. Comparing this with Eq. (32), we see that the unpolarized electron's Wigner function is everywhere positive now, even though the packet is not Gaussian (see Ref. [4]). Treating the term $\mathcal{O}(\hbar)$ as a perturbation, one can also write this via the fully classical current as follows:

$$\begin{aligned}
j^{\mu}_{f\to i}(x) &= \int \frac{d^3p}{(2\pi\hbar)^3}\Bigg\{|\psi|^2 + i|\psi|^2\left(\frac{\partial\varphi}{\partial\mathbf{p}} - \left\langle\frac{\partial\varphi}{\partial\mathbf{p}}\right\rangle\right)\hat{\mathbf{p}}\\
&\quad + \frac{1}{4}\left[D_{ij} - 2|\psi|^2\left(\frac{\partial\varphi}{\partial p_i} - \left\langle\frac{\partial\varphi}{\partial p_i}\right\rangle\right)\left(\frac{\partial\varphi}{\partial p_j} - \left\langle\frac{\partial\varphi}{\partial p_j}\right\rangle\right)\right]\hat{p}_i\hat{p}_j + \mathcal{O}(\hbar^3)\Bigg\}j^{\mu}_{\text{cl.}}(\mathbf{x},\mathbf{p},t),\\
j^{\mu}_{\text{cl.}}(\mathbf{x},\mathbf{p},t) &= \frac{p^{\mu}}{\varepsilon}\,\delta(\mathbf{x} - \mathbf{u}t).
\end{aligned} \tag{40}$$

Depending on the boundary conditions, the rectilinear motion here corresponds either to Cherenkov radiation or to transition radiation, etc. A generalization of this for arbitrary classical motion in a given field is obvious:

$$\mathbf{u}t \to \mathbf{r}(t).$$

Thus the transition current represents a functional of the classical current and of the classical trajectory [7–9] and its quantum corrections due to the recoil are proportional to $\hbar$ and depend on the derivatives of the packet's phase. Remarkably, even when the recoil is vanishing ($\hbar\omega/\varepsilon \to 0$) the current still represents a superposition of trajectories with the different momenta [7,8] defined by the wave function $|\Psi|^2$, about which we have not made any assumptions. If this function is, for instance, of a Gaussian form,

$$|\Psi|^2 \propto \exp\left\{-\frac{(\mathbf{p} - \langle\mathbf{p}\rangle)^2}{(\delta p)^2}\right\}, \tag{41}$$

the current is equal to

$$j^{\mu}_{f\to i}(x) = j^{\mu}_{\text{cl.}}(\mathbf{x},\langle\mathbf{p}\rangle,t) + \mathcal{O}\left(\frac{(\delta p)^2}{m^2}\right), \tag{42}$$

and it acquires an inherently quantum *nonparaxial correction* [39]

$$\frac{(\delta p)^2}{m^2} = \frac{\lambda_c^2}{\sigma_\perp^2} \ll 1 \tag{43}$$

due to the packet's finite size $\sigma_\perp = \hbar/\delta p$. Thus this size can influence the radiation, although only when the packet is very narrow, $\sigma_\perp \gtrsim \lambda_c$, so the ratio $\lambda_c^2/\sigma_\perp^2$ does not exceed 10^{-6} for relevant parameters. It is these corrections that are neglected in such quasiclassical methods as, for instance, the operator method [13,14] or the eikonal approximation [8].

The packet's shape, defined by the phase φ, influences the first quantum correction to the current but not the leading term. An important exception here, however, is the vortex electrons because for them [19,39]

$$|\psi|^2 \propto p_\perp^{2|\ell|},$$

and the transition current depends on *the absolute value* of the electron OAM $|\ell|$ already in the leading order, which results in an enhancement of the nonparaxial correction (43) [39]:

$$\lambda_c^2/\sigma_\perp^2 \to |\ell|\,\lambda_c^2/\sigma_\perp^2. \tag{44}$$

Let us now derive a more general expression for the current, which allows one to study two opposite limiting cases: (1) a delocalized plane-wave electron and (2) a pointlike classical particle. We suppose that the electron wave function has a Gaussian envelope, analogously to Eq. (16):

$$\psi(\mathbf{p}) = \tilde{\psi}(\mathbf{p})\,\exp\left\{-\frac{(\mathbf{p} - \langle\mathbf{p}\rangle)^2}{2(\delta p)^2}\right\},\ \tilde{\psi}(\mathbf{p}) = |\tilde{\psi}|\,e^{i\varphi}. \tag{45}$$

Then instead of the delta function the integral over $\mathbf{q}$ yields the following result:

$$\begin{aligned}
j^{\mu}_{f\to i}(x) &= \frac{(\delta p)^3}{\pi^{3/2}\hbar^3}\int \frac{d^3p}{(2\pi\hbar)^3}\,\frac{p^{\mu}}{\varepsilon}\Bigg(|\tilde{\psi}|^2 + \frac{(\delta p)^2}{2}\Bigg\{\mathrm{Tr}\,D_{ij} - 2\sigma_\perp^{-2}\left[\mathbf{x} - \mathbf{u}t + \hbar\left(\frac{\partial\varphi}{\partial\mathbf{p}} - \left\langle\frac{\partial\varphi}{\partial\mathbf{p}}\right\rangle\right)\right]_i\\
&\quad\times\left[\mathbf{x} - \mathbf{u}t + \hbar\left(\frac{\partial\varphi}{\partial\mathbf{p}} - \left\langle\frac{\partial\varphi}{\partial\mathbf{p}}\right\rangle\right)\right]_j D_{ij}\Bigg\} + \mathcal{O}[(\delta p)^4]\Bigg)\exp\left\{-\frac{(\mathbf{p} - \langle\mathbf{p}\rangle)^2}{(\delta p)^2} - \sigma_\perp^{-2}\left[\mathbf{x} - \mathbf{u}t + \hbar\left(\frac{\partial\varphi}{\partial\mathbf{p}} - \left\langle\frac{\partial\varphi}{\partial\mathbf{p}}\right\rangle\right)\right]^2\right\},
\end{aligned} \tag{46}$$

where $\sigma_\perp = \hbar/\delta p = \mathcal{O}(\hbar)$. When $\sigma_\perp \to 0$ (or $\hbar \to 0$) for arbitrary δp, we return to Eq. (40). However when $\delta p \to 0$ for nonvanishing $\sigma_\perp$, we have

$$j^\mu_{f\to i}(x) = \text{const}\, |\tilde{\psi}(\langle \mathbf{p}\rangle)|^2 \, \frac{\langle p\rangle^\mu}{\varepsilon} \equiv \frac{1}{V}\,\frac{\langle p\rangle^\mu}{\langle \varepsilon\rangle}, \tag{47}$$

which is a delocalized current of the plane-wave state:

$$\psi(x) = (2\langle\varepsilon\rangle V)^{-1/2}\, u_i(\langle p\rangle) \exp\{-i\langle p\rangle x\}. \tag{48}$$

We now return to Eq. (40) and notice that the first correction due to recoil in the matrix element $S_{fi} = -ie\int d^4x\, j^\mu_{fi}(x) A^*_\mu(x)$ looks as follows after the integration by parts (we again omit $\hbar$):

$$S_{fi} \propto ie \int d^4x \frac{d^3p}{(2\pi)^3}\, |\psi|^2 \left(\frac{\partial\varphi}{\partial\mathbf{p}} - \left\langle \frac{\partial\varphi}{\partial\mathbf{p}}\right\rangle\right) \times j^\mu_{\text{cl.}}(\mathbf{x},\mathbf{p},t)\, \nabla A^*_\mu(x)|_{\mathbf{x}=\mathbf{u}t}. \tag{49}$$

Analogously, the second quantum correction contains

$$\nabla_i \nabla_j A^*_\mu(x)|_{\mathbf{x}=\mathbf{u}t}.$$

Thus we see that the series in powers of the recoil—that is, ω/ε—automatically generates a multipole series in the matrix element. In particular, the second correction in Eq. (40) depends on

$$(\partial\varphi/\partial p_i)(\partial\varphi/\partial p_j)$$

and, therefore, on the packet's *electric quadrupole moment* [19,20]. For a plane-wave photon, we have $\nabla A^*_\mu(x)|_{\mathbf{x}=\mathbf{u}t} = -i\mathbf{k}A^*_\mu(t,\mathbf{u}t)$. The radiation intensity dW defined by $|S_{fi}|^2$ thus includes the leading classical term and two sorts of quantum corrections: (1) those due to the recoil, which also depend on the packet's multipole moments due to the phase φ, and (2) the nonparaxial corrections due to the packet's finite size. The intensity also depends on the interference between the multipole contributions—see Eq. (3). Importantly, these conclusions hold both (i) for radiation of an accelerated electron in an external field and (ii) when the particle interacts with a medium and no acceleration is required (Cherenkov radiation, transition radiation, Smith-Purcell radiation, etc.).

Finally, when the packet's quantum numbers, which define its shape, are large, we can neglect the terms of the order of ω/ε compared to the contribution from the phase φ, as we noted in the beginning of this section. Say, for a vortex electron we have

$$\varphi = \ell\phi$$

and the first quantum correction to the current and to the matrix element *depends on the sign* of the OAM ℓ via $\partial\varphi/\partial\mathbf{p}$. One can retrieve this magnetic dipole contribution by the following asymmetry:

$$\frac{dW(\ell) - dW(-\ell)}{dW(\ell) + dW(-\ell)} = \frac{dW_{e\mu}}{dW_e} = \mathcal{O}\Big(\ell\frac{\omega}{\varepsilon}\Big), \tag{50}$$

analogously to Ref. [37], which is ℓ times larger than the corresponding spin asymmetry for a Gaussian packet. Likewise, the quadrupole contribution without the spreading is attenuated as $\ell^2\lambda_c^2/\sigma_\perp^2$ (see the next section), which can also be much larger than ω/ε for $|\ell| \gg 1$. Compared to the quasiclassical regime of emission by relativistic particles [8,13], in which the electron motion is classical but the recoil is kept, here we have the opposite situation: the recoil is vanishing but the effects due to non-Gaussianity of the electron packet are enhanced.

Before we come to calculations of the Smith-Purcell radiation, we emphasize that while the above first-order QED approach is applicable not only to processes in the given external fields but also to radiation in a given medium, the diffraction radiation and Smith-Purcell radiation from a conducting grating *cannot, strictly speaking, be described in a model-independent way* within the first order of the perturbation theory in QED. This is because we either have to take the incident field of the moving electron as given (that is, to neglect the electron's recoil) and to consider radiation of the induced surface current (as in Refs. [17,25,27,28,31,40,41]) or to take a given surface wave and to consider radiation of the electron in its field (as in Refs. [2,5]), that is, to neglect the recoil of the surface wave. Clearly, the predictions of both these phenomenological approaches can be different, exactly as they are so already in the classical framework (see Ref. [30]). In what follows, we rely on the former (surface current) approach, the validity of which was experimentally verified for diffraction radiation and Smith-Purcell radiation (see, for instance, Ref. [42]) and which is a limiting case of a more general polarization current method, applicable for arbitrary permittivity [28].

IV. SMITH-PURCELL RADIATION FROM A VORTEX PACKET

Here we study how quantum dynamics of the emitting electron packet—that is, nonvanishing $\langle\rho\rangle(t)$—influences the radiation characteristics. A freely propagating packet always spreads, but this does not affect the radiation intensity for packets that are Gaussian in the rest frame with the equal transverse and longitudinal uncertainties, $\sigma_\perp^{(e)} = \sigma_{||}^{(e)}$, because for such packets all the higher multipole moments are vanishing [19] and the particle radiates as if its charge were confined to a point, $dW = dW_e$. The packets that are either non-Gaussian or nonsymmetric in the rest frame, $\sigma_\perp^{(e)} \neq \sigma_{||}^{(e)}$, can possess a magnetic dipole moment, an electric quadrupole moment, and so on. For such packets there appear additional terms in Eq. (3) because the far-field intensity dW is generally sensitive to the size of the electron packet and to its shape defined by the phase $\varphi(\mathbf{p})$ of the wave function. The vortex electrons with OAM ℓ [18], the Airy beams [24], as well as coherent superpositions of states can serve as such non-Gaussian packets and they also have an electric quadrupole moment, which—unlike the magnetic moment—has a finite radius defined by the packet's coherence length. Importantly, the quadrupole contribution comes about only *beyond the paraxial approximation* [39], which implies that the packet is narrow (unlike that of Ref. [2]) and the OAM is large $\ell \gg 1$. In this nonparaxial regime, an electron radiates in the far field as if it had its charge spread over the entire region of $\sigma_\perp^{(e)}$, while the contribution depending on the coherence length can be *nonlinearly enhanced.*

Consider Smith-Purcell radiation generated by a nonrelativistic vortex electron moving with a mean momentum $\langle p\rangle = \beta m$ along the z axis at the impact parameter h with respect to an ideally conducting grating of N strips with a period d (see Fig. 2). The vortex electron is described as *a generalized (nonparaxial) Laguerre-Gaussian packet* [39,43]:

$$\psi_{\ell,n}(\boldsymbol{x},t) = \sqrt{\frac{n!}{(n+|\ell|)!}}\,\frac{i^{2n+\ell}}{\pi^{3/4}}\,\frac{\rho^{|\ell|}}{(\sigma_\perp^{(e)}(t))^{|\ell|+3/2}}\,L_n^{|\ell|}\left(\frac{\rho^2}{(\sigma_\perp^{(e)}(t))^2}\right)\exp\bigg\{-it\langle p\rangle^2/2m + i\langle p\rangle z + i\ell\phi_r$$
$$- i(2n+|\ell|+3/2)\arctan(t/t_d) - \frac{1}{2(\sigma_\perp^{(e)}(t))^2}(1-it/t_d)[\rho^2+(z-\langle u\rangle t)^2]\bigg\},$$
$$\int d^3x\,|\psi_{\ell,n}(\boldsymbol{x},t)|^2 = 1,\ \sigma_\perp^{(e)}(t) = \sigma_\perp^{(e)}\sqrt{1+t^2/t_d^2}, \tag{51}$$

which is an exact solution to the Schrödinger equation and where $\lambda_c = 1/m \approx 3.9\times10^{-11}$ cm is the Compton wavelength, and t_d is an effective diffraction time. The difference of this nonparaxial solution from the paraxial (approximate solution) Laguerre-Gaussian packets described in Ref. [18] is important for nonrelativistic particles due to symmetry properties of the Gouy phase and the *CPT* theorem [39,43]. Here, $L_n^{|\ell|}$ are associated Laguerre polynomials; $n = 0, 1, 2, \ldots$ defines the number of radial maxima; and in what follows we study the case $n = 0$ with one maximum only. The magnetic moment and the electric quadrupole moment of such a vortex packet are [19,20,43]

$$\boldsymbol{\mu} = \hat{z}\,\frac{\ell}{2m},\quad Q_{ij}(t) = |\ell|\,[\sigma_\perp^{(e)}(t)]^2\,\mathrm{diag}\{1/2, 1/2, -1\}. \tag{52}$$

The mean radius of such a packet is $\sqrt{|\ell|}$ times larger than $\sigma_\perp^{(e)} \equiv \sigma_{||}^{(e)}$ [39,44]:

$$\langle\rho\rangle \approx \sqrt{|\ell|}\,\sigma_\perp^{(e)}. \tag{53}$$

Neglecting both the recoil and the quadratic corrections dW_μ, dW_Q, etc., we have the following radiation intensity:

$$dW = dW_e + dW_{e\mu} + dW_{eQ}, \tag{54}$$

where neither dW_e nor $dW_{e\mu}$ depends on the packet's width, but dW_{eQ} does. We calculate these terms according to the model in Ref. [31] in which the surface current density

$$\boldsymbol{j}_s(\boldsymbol{x},\omega) = \frac{1}{2\pi}\,\boldsymbol{e}_k\times[\boldsymbol{n}\times\boldsymbol{E}(\boldsymbol{x},\omega)] \tag{55}$$

is induced by the given field

$$\boldsymbol{E} = \boldsymbol{E}_e + \boldsymbol{E}_\mu + \boldsymbol{E}_Q \tag{56}$$

of the first three moments of the vortex packet (51) derived in Ref. [43]. Here $\boldsymbol{n}$ is a unit vector normal to the grating (see Fig. 2), and $\boldsymbol{e}_k = \{\sin\Theta\cos\Phi, \sin\Theta\sin\Phi, \cos\Theta\}$. The radiation field in the wave zone and the intensity are [31]

$$\boldsymbol{E}^R = i\omega\,\frac{e^{ir_0\omega}}{r_0}\int_S d^2x\,\boldsymbol{j}_s(\boldsymbol{x},\omega)\,e^{-i\boldsymbol{k}\boldsymbol{r}},\quad \frac{d^2W}{d\omega d\Omega} = r_0^2\,|\boldsymbol{E}^R|^2, \tag{57}$$

where the integration is performed along the surface of the grating and r_0 is a distance to the detector.

The leading (classical) term dW_e is defined by Eqs. (57) and (58) in Ref. [28], while the quantum contribution of the magnetic moment is found as [45]

$$\frac{d^2W_{e\mu}}{d\omega d\Omega} = \frac{\ell}{m}\,\frac{\omega\cos\Phi\sin\Theta(\beta\gamma^2\sin^2\Theta+\cos\Theta)}{\gamma^2(1-\beta\cos\Theta)^2\sqrt{1+\beta^2\gamma^2\cos^2\Phi\sin^2\Theta}}$$
$$\times|F|^2\exp\left(-\frac{4\pi h}{\beta\gamma\lambda}\sqrt{1+\beta^2\gamma^2\cos^2\Phi\sin^2\Theta}\right),$$
$$F = 2\,\frac{\sin\left[\frac{a\omega}{2}(\beta^{-1}-\cos\Theta)\right]}{\omega(\beta^{-1}-\cos\Theta)}\,\frac{\sin\left[\frac{Nd}{2}\omega(\beta^{-1}-\cos\Theta)\right]}{\sin\left[\frac{d}{2}\omega(\beta^{-1}-\cos\Theta)\right]}. \tag{58}$$

When the number of strips is large, $N \gg 1$, the factor F yields a delta function the zeros of which give the Smith-Purcell dispersion relation:

$$\lambda_g = \frac{d}{g}(\beta^{-1}-\cos\Theta),\ g = 1, 2, 3, \ldots. \tag{59}$$

By using this delta function, one can integrate over frequencies, $d^2W/d\omega d\Omega \to dW/d\Omega$. Clearly, the magnetic moment contribution compared to the classical contribution of a charge is attenuated as [see Eq. (50)]

$$\frac{dW_{e\mu}}{dW_e} \sim \ell\,\frac{\omega}{\varepsilon}\cos\Phi, \tag{60}$$

it vanishes at $\Phi = \pi/2$ due to the symmetry considerations in accord with Ref. [37], and it depends on the sign of the OAM. This ratio can reach 10^{-4} for $\ell \sim 10^3$ and $\lambda \sim 1\,\mu$m. Importantly, both dW_e and $dW_{e\mu}$ linearly grow with the number of strips N or with the grating's length $L = Nd$ (see, for instance, Refs. [28,30]).

The next quantum correction due to the quadrupole moment also has a common envelope (5) and it represents a sum of three different terms:

$$dW_{eQ} = dW_{eQ_0} + dW_{eQ_1} + dW_{eQ_2}, \tag{61}$$

where

$$\frac{dW_{eQ_0}}{dW_e} \sim |\ell|\,\frac{(\sigma_\perp^{(e)})^2}{h_{\text{eff}}^2} \text{ — quasiclassical quadrupole contribution,}$$
$$\frac{dW_{eQ_1}}{dW_e} \sim |\ell|\,\frac{\lambda_c^2}{(\sigma_\perp^{(e)})^2} \text{ — nonparaxial quantum correction [39],}$$
$$\frac{dW_{eQ_2}}{dW_e} \sim N^2\,|\ell|\,\frac{\lambda_c^2}{(\sigma_\perp^{(e)})^2} \text{ — dynamically enhanced nonparaxial quantum correction.} \tag{62}$$

Here $h_{\text{eff}} = \beta\gamma\lambda/2\pi$ is denoted. The enhancement of dW_{eQ_2} comes about due to spreading of the packet [see Eq. (51)] and the corresponding integration of the spreading term along the grating in Eq. (57):

$$dW_{eQ} \propto \int dz\,\frac{z^2}{z_R^2} \propto \frac{(Nd)^3}{z_R^2},\; z_R = \beta t_d. \tag{63}$$

When $\sigma_\perp^{(e)} \ll \lambda$, two nonparaxial terms in (62) dominate and we present here only the last one, needed for our purposes. After the integration over frequencies for $N \gg 1$ and for the first diffraction order $g = 1$ it is

$$\frac{dW_{eQ_2}}{d\Omega} = |\ell|\,\frac{\lambda_c^2}{(\sigma_\perp^{(e)})^2}\,\frac{dW_e}{d\Omega}\,\frac{1}{3\beta^4\gamma^4}\,\frac{f(N)}{\lambda_1^2},$$
$$f(N) = 3\pi ad\,\cot\left(\frac{a\pi}{d}\right) + 3\pi^2a^2 + 3\pi\,ad(N-1)$$
$$+ d^2\,[\pi^2(2N^2 - 3N + 1) - 3]$$
$$\approx 2\pi^2d^2N^2 \text{ when } N \gg 1. \tag{64}$$

For very wide packets, $\sigma_\perp^{(e)} \gg \lambda$, the quadratic corrections dW_μ and dW_Q and the higher-order terms in the multipole expansion can become important, which is why we do not consider the case $\sigma_\perp^{(e)} \gtrsim 33\,\mu$m of Ref. [2].

Importantly, both the corrections to dW_e in Eq. (54) have a quantum origin and they vanish for the symmetric Gaussian packet with $\ell = 0$. While $dW_{e\mu}$ is ℓ times larger than the recoil (i.e., $\ell\,\omega/\varepsilon \gg \omega/\varepsilon$, see Ref. [37]), the term dW_{eQ} is due to quantum character of the trajectory [6,9,10,14], which is also supposed to be larger than the recoil. Such geometric corrections can be noticeable for the emission of a coherent superposition of packets with a not-everywhere positive Wigner function [4,11]. However, as we show here, they can also be nonlinearly enhanced due to the spreading, while the recoil stays vanishing, $\omega \ll \varepsilon$, which can take place even for a single-electron state with an everywhere positive Wigner function.

Expectedly, the dynamical contribution (64) is suppressed in relativistic case, $\gamma \gg 1$, when the spreading is marginal or when the radiation formation length is smaller than the Rayleigh length z_R. For nonrelativistic energies, however, the Rayleigh length does not exceed a few cm for relevant parameters and the spreading can noticeably modify the radiation if the length L of the grating of N strips is large: $L = Nd \gg z_R$. For a long grating, $N \gg 1$, the ratio dW_{eQ_2}/dW_e can be only moderately attenuated,

$$dW_{eQ_2}/dW_e \lesssim 1,$$

while both the ordinary nonparaxial contribution and the recoil can still be small:

$$dW_{eQ_1}/dW_e \ll 1,\; \omega/\varepsilon \ll 1.$$

Most importantly, while the classical intensity dW_e linearly grows with the number of strips N, the nonparaxial contribution dW_{eQ_2} grows *nonlinearly* as N^3. This remarkable feature is a direct consequence of the delocalized nature of charge in the spreading twisted packet and it puts an upper limit on the grating length $L_{\max} = N_{\max}d$ for which the radiation losses stay small compared to the particle's energy. This limit can be derived by demanding that both the recoil and the quadratic corrections can be neglected, $\omega/\varepsilon \sim \lambda_c/\lambda \ll dW_{eQ_2}/dW_e \ll 1$, which yields

$$\sqrt{\frac{\lambda_c}{\lambda}}\,\frac{\sigma_\perp^{(e)}}{\lambda_c|\ell|} \ll N \ll \frac{\sigma_\perp^{(e)}}{\lambda_c|\ell|}. \tag{65}$$

For the moderately large OAM, $|\ell| \sim 10$–100, and $\sigma_\perp^{(e)} \sim 1$ nm–1 μm, we have $\sigma_\perp^{(e)}/\lambda_c|\ell| \sim 10$–$10^5$, so the number $N_{\max}$ can be taken as 0.1–0.2 of this value. Note that in contrast to the magnetic moment effects [37], the observation of this nonlinear enhancement does not necessarily require as large an OAM as possible.

The easiest way to detect this nonlinear effect is to perform measurements in the perpendicular plane, around

$$\Theta = \Phi = \pi/2,$$

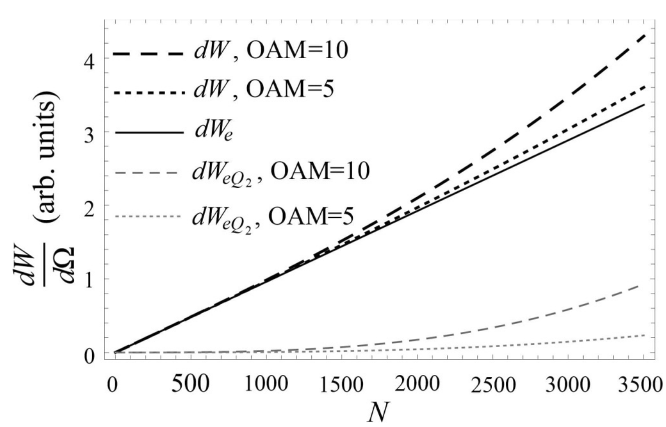

FIG. 3. Dependence of Smith-Purcell radiation on the number of strips for $d = 10\,\mu$m, $\sigma_\perp^{(e)} = 100$ nm, $h = 2.7\,\mu$m, $z_R \approx 1.3$ mm, $N_{\max} \approx 3500$, $L_{\max} \approx 3.5$ cm, $\Theta = \Phi = \pi/2$. While for a point charge this dependence is linear (the solid line), a nonpoint vortex packet with a quadrupole moment reveals an N^3 dependence for $Nd \gg z_R$, where z_R is the Rayleigh length from Eq. (63).

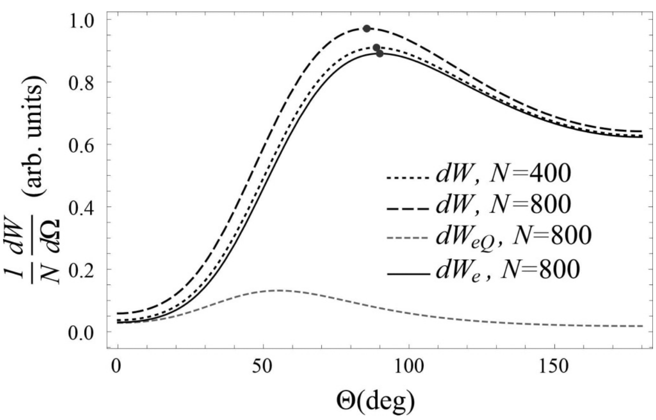

FIG. 4. Polar dependence of Smith-Purcell radiation for $d = 100\,\mu$m, $\sigma_\perp^{(e)} = 20$ nm, $\ell = 10$, $h = 33\,\mu$m, $z_R \approx 70\,\mu$m, $N_{\max} \approx 800$, $L_{\max} \approx 8$ cm, $\Phi = \pi/2$. The maximum (the dot) is shifted due to the quadrupole contribution.

and to compare the radiation from at least three gratings of different length. In this geometry, the magnetic moment term vanishes, $dW_{e\mu} = 0$, and dW_{eQ_2} can reach some 10–20% of the leading term dW_e. The effect can more easily be detected in IR and THz ranges, for which the grating period should be larger than $10\,\mu$m. In Fig. 3 we present the nonlinear growth of the intensity with the number of strips, which can be seen with the naked eye, while in Fig. 4 the enhancement for the small polar angles,

$$dW_{eQ_2}(\Theta = 0)/dW_{eQ_2}(\Theta = \pi/2) \approx 4,$$

is shown accompanied with a several-degree shift of the maximum. If detected, this shift could also serve as an evidence of the quadrupole contribution.

As the electron coherence length in the vicinity of a cathode does not exceed a few nm [46,47] and for vortex packets it scales as $\sigma_\perp^{(e)} \propto \sqrt{|\ell|}$, the grating must be placed not too far from the vortex electron source or, alternatively, the focusing can be applied. When detecting many photons from electrons of a beam, it is important to have the beam angular divergence as small as possible, otherwise many electrons could hit the grating well before they reach the part where the quadrupole contribution becomes noticeable. For the optical range and the grating period $d = 416$ nm, the maximal grating length $L_{\max} \sim 10\,\mu$m matches the effective interaction length of the beam used in Ref. [2] (the distance before an electron hits the grating) for $\sigma_\perp^{(e)} \sim 10$ nm and $|\ell| \sim 200$, which seems feasible, although the beam focusing could be needed. Instead of minimizing the beam divergence, one could also rotate the grating so as to minimize the electron losses, although at the expense of statistics.

The above nonlinear enhancement can also reveal itself in other processes with the nonrelativistic non-Gaussian packets for which the radiation formation length can be much larger than the Rayleigh length, such as Cherenkov radiation and diffraction radiation in a cylindrical channel of a finite length, transition radiation in a slab, Compton emission in a laser pulse, and so on.

V. CONCLUSION

Concluding, we have argued that the classical prewave zone effect could have been the reason for the wide azimuthal distributions of Smith-Purcell radiation reported in Ref. [2]. The continuous current density interpretation of the wave function can still be used when the radiation intensity depends on the electron coherence length, which is generally the case but mostly for nonrelativistic electrons. Taking the same example of Smith-Purcell radiation, we have predicted a nonlinear enhancement of the quantum nonparaxial corrections to the classical radiation intensity due to the nonlocal nature of charge in a spreading packet of the vortex electron. Moreover, any nonrelativistic and non-Gaussian or highly nonsymmetric packet with an electric quadrupole moment can emit radiation in the far field as if its charge were spread over the entire coherence length. This nonpoint contribution can reveal itself in a nonlinear growth of the intensity for a family of emission processes when the radiation formation length exceeds the Rayleigh length. Our findings support Bohr's complementarity principle and demonstrate that a choice between the two seemingly contradictory interpretations of a square modulus of the wave function depends on the experimental conditions, in particular, on a distance to the detector, and on a quantum state and energy of the projectile.

ACKNOWLEDGMENTS

We are grateful to A. Aryshev, V. G. Bagrov, A. P. Potylitsyn, and, especially, P. O. Kazinski and A. A. Tishchenko for fruitful discussions and criticism. This work is supported by the Russian Science Foundation (Project No. 17-72-20013).

[1] L. de Broglie, Recherches sur la théorie des quanta, Thése de doctorat soutenue Paris le 25 novembre 1924, Ann. Phys. (Paris) **3**, 22 (1925).
[2] R. Remez, A. Karnieli, S. Trajtenberg-Mills, N. Shapira, I. Kaminer, Y. Lereah, and A. Arie, Observing the Quantum Wave Nature of Free Electrons through Spontaneous Emission, Phys. Rev. Lett. **123**, 060401 (2019).
[3] S. J. Smith and E. M. Purcell, Visible light from localized surface charges moving across a grating, Phys. Rev. **92**, 1069 (1953).
[4] J. Peatross, C. Müller, K. Z. Hatsagortsyan, and C. H. Keitel, Photoemission of a Single-Electron Wave Packet in a Strong Laser Field, Phys. Rev. Lett. **100**, 153601 (2008).
[5] Y. Pan and A. Gover, Spontaneous and stimulated emissions of a preformed quantum free-electron wave function, Phys. Rev. A **99**, 052107 (2019).
[6] A. A. Sokolov and I. M. Ternov, in *Radiation from Relativistic Electrons*, edited by C. W. Kilmister, American Institute of Physics Translation Series (AIP, New York, 1986).
[7] A. I. Akhiezer and N. F. Shul'ga, A theory of relativistic particle radiation in the quasi-classical approximation, Phys. Lett. A **144**, 415 (1990).

[8] A. I. Akhiezer and N. F. Shul'ga, Semiclassical theory of high-energy particle radiation in external fields, Phys. Rep. **234**, 297 (1993).
[9] V. G. Bagrov, V. V. Belov, and A. Yu. Trifonov, Theory of spontaneous radiation by electrons in a trajectory-coherent approximation, J. Phys. A: Math. Gen. **26**, 6431 (1993).
[10] V. V. Belov, D. V. Boltovskiy, and A. Yu. Trifonov, Theory of spontaneous radiation by bosons in quasiclassical trajectory-coherent approximation, Int. J. Mod. Phys. B **8**, 2503 (1994).
[11] A. Angioi and A. Di Piazza, Quantum Limitation to the Coherent Emission of Accelerated Charges, Phys. Rev. Lett. **121**, 010402 (2018).
[12] E. Wigner, On the quantum correction for thermodynamic equilibrium, Phys. Rev. **40**, 749 (1932).
[13] V. N. Baier and V. M. Katkov, Processes involved in the motion of high energy particles in a magnetic field, Zh. Eksp. Teor. Fiz. **53**, 1478 (1967) [Sov. Phys. JETP **26**, 854 (1968)]; Quasiclassical theory of bremsstrahlung by relativistic particles, **55**, 1542 (1968) [**28**, 807 (1969)].
[14] V. B. Berestetskii, E. M. Lifshitz, and L. P. Pitaevskii, *Quantum Electrodynamics* (Pergamon Press, New York, 1982).
[15] V. A. Verzilov, Transition radiation in the pre-wave zone, Phys. Lett. A **273**, 135 (2000).
[16] D. V. Karlovets and A. P. Potylitsyn, Smith Purcell radiation in the pre-wave zone, JETP Lett. **84**, 489 (2006).
[17] A. P. Potylitsyn, M. I. Ryazanov, M. N. Strikhanov, and A. A. Tishchenko, *Diffraction Radiation from Relativistic Particles*, Springer Tracts in Modern Physics Vol. 239 (Springer-Verlag, Berlin, 2010).
[18] K. Y. Bliokh, I. P. Ivanov, G. Guzzinati, L.Clark, R. Van Boxem, A.Béché, R. Juchtmans, M. A. Alonso, P. Schattschneider, F. Nori, J. Verbeeck *et al.*, Theory and applications of free-electron vortex states, Phys. Rep. **690**, 1 (2017).
[19] D. Karlovets and A. Zhevlakov, Intrinsic multipole moments of non-Gaussian wave packets, Phys. Rev. A **99**, 022103 (2019).
[20] A. J. Silenko, P. Zhang, and L. Zou, Electric Quadrupole Moment and the Tensor Magnetic Polarizability of Twisted Electrons and a Potential for Their Measurements, Phys. Rev. Lett. **122**, 063201 (2019).
[21] H. L. Andrews and C. A. Brau, Gain of a Smith-Purcell free-electron laser, Phys. Rev. Spec. Top.: Accel. Beams **7**, 070701 (2004).
[22] H. L. Andrews, C. H. Boulware, C. A. Brau, and J. D. Jarvis, Dispersion and attenuation in a Smith-Purcell free electron laser, Phys. Rev. Spec. Top.: Accel. Beams **8**, 050703 (2005).
[23] N. Talebi, Schrödinger electrons interacting with optical gratings: Quantum mechanical study of the inverse Smith Purcell effect, New J. Phys. **18**, 123006 (2016).
[24] N. Voloch-Bloch, Y. Lereah, Y. Lilach, A. Gover, and A. Arie, Generation of electron Airy beams, Nature (London) **494**, 331 (2013).
[25] A. P. Kazantsev and G. I. Surdutovich, Sov. Phys. Dokl. **7**, 990 (1963).
[26] A. P. Potylitsyn, Resonant diffraction radiation and Smith-Purcell effect, Phys. Lett. A **238**, 112 (1998).
[27] J. H. Brownell, J. Walsh, and G. Doucas, Spontaneous Smith-Purcell radiation described through induced surface currents, Phys. Rev. E **57**, 1075 (1998).
[28] D. V. Karlovets, On the theory of polarization radiation in media with sharp boundaries, J. Exp. Theor. Phys. **113**, 27 (2011).
[29] We neglect the spin. The electron's electric dipole moment is prohibited in the standard model [14].
[30] D. V. Karlovets and A. P. Potylitsyn, Comparison of Smith-Purcell radiation models and criteria for their verification, Phys. Rev. Spec. Top.: Accel. Beams **9**, 080701 (2006).
[31] D. V. Karlovets and A. P. Potylitsyn, Generalized surface current method in the macroscopic theory of diffraction radiation, Phys. Lett. A **373**, 1988 (2009).
[32] J. D. Jackson, *Classical Electrodynamics* (Wiley, New York, 1999).
[33] D. V. Karlovets and V. G. Serbo, Effects of the transverse coherence length in relativistic collisions, Phys. Rev. D **101**, 076009 (2020).
[34] The lack of the dependence on the phase $\varphi(\mathbf{p})$ when both the final particles are the plane waves looks very natural: this phase defines the shape of the incoming packet. But if the current $j^{\mu}_{fi}(x)$ is not localized such a shape does not have a sense.
[35] G. L. Kotkin and V. G. Serbo, Beam-size effect at colliders and correlations of particles in a beam, Phys. Rev. Spec. Top.: Accel. Beams **7**, 101001 (2004).
[36] A. A. Tishchenko and D. Yu. Sergeeva, Incoherent Form Factor in Diffraction and Smith-Purcell Radiations, JETP Lett. **110**, 638 (2019).
[37] I. P. Ivanov and D. V. Karlovets, Detecting Transition Radiation from a Magnetic Moment, Phys. Rev. Lett. **110**, 264801 (2013); I. P. Ivanov, Polarization radiation of vortex electrons with large orbital angular momentum, Phys. Rev. A **88**, 043840 (2013).
[38] It is clear from the Gordon identity, $\bar{u}(\mathbf{p}-\mathbf{q}/2)\gamma^{\mu}u(\mathbf{p}+\mathbf{q}/2) = \frac{1}{2m}\bar{u}(\mathbf{p}-\mathbf{q}/2)(2p^{\mu} - i\sigma^{\mu\nu}q_{\nu})u(\mathbf{p}+\mathbf{q}/2)$.
[39] D. Karlovets, Relativistic vortex electrons: Paraxial versus nonparaxial regimes, Phys. Rev. A **98**, 012137 (2018).
[40] M. I. Ryazanov and I. S. Tilinin, Transition radiation emitted by an ultrarelativistic particle crossing a curved interface between media, Zh. Eksp. Teor. Fiz. **71**, 2078 (1976) [Sov. Phys. JETP **44**, 1092 (1976)].
[41] A. G. Shkvarunets and R. B. Fiorito, Phys. Rev. Spec. Top.: Accel. Beams **11**, 012801 (2008).
[42] V. Blackmore, G. Doucas, C. Perry, B. Ottewell, M. F. Kimmitt, M. Woods, S. Molloy, and R. Arnold, First measurements of the longitudinal bunch profile of a 28.5 GeV beam using coherent Smith-Purcell radiation, Phys. Rev. Spec. Top.: Accel. Beams **12**, 032803 (2009).
[43] D. Karlovets, Dynamical enhancement of nonparaxial effects in the electromagnetic field of a vortex electron, Phys. Rev. A **99**, 043824 (2019).
[44] M. Krenn and A. Zeilinger, On small beams with large topological charge: II. Photons, electrons and gravitational waves, New J. Phys. **20**, 063006 (2018).
[45] This formula and Eq. (64) below are also valid for the relativistic electron with $\gamma \gg 1$ as we use the fields $\boldsymbol{E}$ in the laboratory frame from Ref. [43].
[46] B. Cho, T. Ichimura, R. Shimizu, and C. Oshima, Quantitative Evaluation of Spatial Coherence of the Electron Beam from Low Temperature Field Emitters, Phys. Rev. Lett. **92**, 246103 (2004).
[47] D. Ehberger, J. Hammer, M. Eisele, M. Krüger, J. Noe, A. Högele, and P. Hommelhoff, Highly Coherent Electron Beam from a Laser-Triggered Tungsten Needle Tip, Phys. Rev. Lett. **114**, 227601 (2015).